THE JOURNAL OF BIOLOGICAL CHEMISTRY VOL. 283, NO. 52, pp. 36257–36264, December 26, 2008

Mesodermal Deletion of Transforming Growth Factor-β Receptor II Disrupts Lung Epithelial Morphogenesis

*CROSS-TALK BETWEEN TGF-β AND SONIC HEDGEHOG PATHWAYS**

Received for publication, September 2, 2008, and in revised form, October 22, 2008 Published, JBC Papers in Press, November 6, 2008, DOI 10.1074/jbc.M806786200

Min Li[‡], Changgong Li[‡], Yi-hsin Liu[§], Yiming Xing[‡], Lingyan Hu[‡], Zea Borok[¶], Kenny Y.-C. Kwong[‡], and Parviz Minoo[‡1]

From the [‡]Division of Neonatology, Department of Pediatrics, the [§]Department of Ophthalmology, and the [¶]Will Rogers Institute Pulmonary Research Center, Department of Medicine, University of Southern California Schools of Medicine, Los Angeles, California 90033

In vertebrates, Sonic hedgehog (Shh) and transforming growth factor-β (TGF-β) signaling pathways occur in an overlapping manner in many morphogenetic processes. *In vitro* data indicate that the two pathways may interact. Whether such interactions occur during embryonic development remains unknown. Using embryonic lung morphogenesis as a model, we generated transgenic mice in which exon 2 of the *TβRII* gene, which encodes the type II TGF-β receptor, was deleted via a mesodermal-specific Cre. Mesodermal-specific deletion of *TβRII* (*TβRII*$^{\Delta/\Delta}$) resulted in embryonic lethality. The lungs showed abnormalities in both number and shape of cartilage in trachea and bronchi. In the lung parenchyma, where epithelial-mesenchymal interactions are critical for normal development, deletion of mesenchymal *TβRII* caused abnormalities in epithelial morphogenesis. Failure in normal epithelial branching morphogenesis in the *TβRII*$^{\Delta/\Delta}$ lungs caused cystic airway malformations. Interruption of the *TβRII* locus in the lung mesenchyme increased mRNA for *Patched* and *Gli-1*, two downstream targets of Shh signaling, without alterations in Shh ligand levels produced in the epithelium. Therefore, we conclude that TβRII-mediated signaling in the lung mesenchyme modulates transduction of Shh signaling that originates from the epithelium. To our knowledge, this is the first *in vivo* evidence for a reciprocal and novel mode of cross-communication between Shh and TGF-β pathways during embryonic development.

Transforming growth factor-β (TGF-β)[2] ligands are multifunctional signaling proteins that exhibit a wide range of biological activities including regulation of cell proliferation and differentiation. TGF-β initiates its cellular actions by interacting with a heteromeric complex of transmembrane serine/threonine kinase receptors, the type I (TβRI) and type II (TβRII) receptors. The binding of TGF-β ligand to the receptor complex induces phosphorylation of type I by the type II receptors and activates Smads, a family of transcriptional factors that act as intracellular effectors of TGF-β signaling (1). Smad*2* and/or Smad3 are phosphorylated in their C-terminal domain upon stimulation by either activin or TGF-β (2). Phosphorylation of Smad*2* and Smad3 is accompanied by their association with Smad4 and translocation of the heteromeric complex to the nucleus where they affect transcription of target genes through interaction with promoter-specific transcriptional factors or by direct DNA binding (3).

Genetic manipulations of endogenous TGF-β signaling have revealed their important functions in vertebrate development. Targeted deletion of each of the three ligand isoforms causes severe abnormalities in morphogenesis of various organs including the lung. *Tgf-β2*-null mice exhibit perinatal mortality and a wide range of developmental abnormalities that include cardiac, lung, craniofacial, limb, spinal column, eye, inner ear, and urogenital defects (4). *Tgf-β3* mutants die as neonates due to abnormal lung development and cleft palate (5). Targeted disruption of the *Tgf-β1* gene results in abnormalities in the lung, manifested as dilation of the airways (6). Mice with targeted deletion of *Smad3* are viable, but develop lung abnormalities akin to emphysema (7). Little is known about the role of other components of the TGF-β pathway and interactions with other signaling molecules in the lung.

Embryonic lung development represents a useful model in which to study complex tissue interactions in organ development. Lung morphogenesis is strictly dependent on cross-talk between two distinct tissues, the endodermal-derived epithelium and the mesodermal-derived lung mesenchyme (8). A major signaling pathway in this communication is *Shh*, the vertebrate homologue of Drosophila *hh*, which is highly expressed by embryonic lung epithelium. Patched (Ptc), the receptor for Shh is expressed by the lung mesenchyme, the site of highly focalized Fgf10 production. The role of Fgf10 in directing epithelial morphogenesis is central to lung development (9–12). In *Fgf10*(−/−) embryos, the lung tissue below the main stem bronchi is entirely absent (13, 14). Shh interacts with the Ptc/Smoothened (Smo) complex on the mesenchymal cell membrane and activates Gli-3, a 190-kDa transcription factor (15, 16). Activated Gli-3 binds directly to the *Gli-1* promoter and induces its transcription in response to Shh (17). Gli-1 is a zinc transcription factor that activates the transcription of *Ptc* (18).

* This work was supported, in whole or in part, by NHLBI, National Institutes of Health. This work was also supported by the Hastings Foundation. The costs of publication of this article were defrayed in part by the payment of page charges. This article must therefore be hereby marked "*advertisement*" in accordance with 18 U.S.C. Section 1734 solely to indicate this fact.

[1] To whom correspondence should be addressed: General Laboratories Bldg. 1801 E. Marengo St., Rm. 1G1, Los Angeles, CA 90033. Tel.: 323-226-4340; Fax: 323-226-5049; E-mail: minoo@usc.edu.

[2] The abbreviations used are: TGF, transforming growth factor; X-gal, 5-bromo-4-chloro-3-indolyl-β-D-galactopyranoside; Shh, Sonic hedgehog; PBSMC, parabronchial smooth muscle cells; GAPDH, glyceraldehyde-3-phosphate dehydrogenase.

Thus, increased transcription of *Gli-1* & *Ptc* are reliable markers of Shh pathway activation. All three *Gli* family members are expressed in and are important for lung development (18, 19). The currently accepted model is that Shh both stimulates and restricts the level and spatial distribution of *Fgf10* expression during lung morphogenesis. Consistent with this concept, deletion of *Shh* leads to diffused, but expanded *Fgf10* mRNA throughout the mesenchyme as a consequence of which airways develop into large cystic structures (20). Precisely how Shh controls *Fgf10* gene expression has hitherto remained unknown.

Because of its established role as a negative regulator of lung branching morphogenesis (21) TGF-β is a potential mediator in epithelial-mesenchymal cross-talk during lung development. Conventional deletion of *TβRII* lead to early embryonic lethality, and therefore was not informative for lung development (22). In the present study, we used a mesodermal-specific *cre-loxP* system to delete exon 2 in the *TβRII* locus in the lung mesenchyme. The lungs of $T\beta RII^{\Delta/\Delta}$ mouse fetuses are abnormal with evidence of cystic airway malformations associated with alterations in *Fgf10* gene expression, likely due to interruption of normal epithelial-mesenchymal cross-talk. Inactivation of *TβRII* and hence the specific TGF-β signaling pathway mediated through its normal activity in the lung mesenchyme results in alterations in *Ptc* and *Gli* mRNAs in the mutant lungs indicating interference with Shh signaling. Thus, TGF-β signaling, mediated via TβRII can modulate mesenchymal reception of Shh signaling, which originates from the epithelium, indicating cross-communication between the two signaling pathways during embryonic lung morphogenesis.

MATERIALS AND METHODS

Animals—Dermo1-cre, Rosa26-lacZ, and $T\beta RII^{fl/fl}$ mice were generated and genotyped as previously described (23–25) and maintained on C57BL/6 genetic background. *Dermo1-cre; Rosa26-lacZ* mice were generated by crossing *Dermo1-* and *Rosa26-lacZ* mice. To generate $T\beta RII^{fl/fl}$*; Dermo1-cre* embryos ($T\beta RII^{\Delta/\Delta}$), $T\beta RII^{fl/+}$*; Derom1-cre* mice were crossed with $T\beta RII^{fl/fl}$ mice.

Detection of β-Galactosidase (LacZ) Activity—LacZ activity was determined by X-gal staining as described (26). Whole mount staining was performed for embryonic lungs. Lungs of E15.5 and older were fixed and sectioned by cryostat, and the frozen sections were stained for LacZ activity.

Immunohistochemistry—For immunohistochemistry, samples were fixed in 4% paraformaldehyde and processed into serial paraffin sections using routine procedures. Immunostaining were performed as previously described (27). Primary antibodies that were used are: α-SMA (Sigma), PAI-1 (Abcam Cambridge, MA), PECAM (BD Pharmingen, San Diego, CA), Flk1 (Cell Signaling Technology, Beverly, MA), β-Tubulin (Biogenix, San Ramon, CA), Collagen1 (Abcam, Cambridge, MA), and TβRII (Abcam Cambridge, MA).

Western Blot Analysis—Protein extracts were prepared from E15.5 *Dermo1-cre;* $T\beta RII^{fl/fl}$ and $T\beta RII^{\Delta/\Delta}$ lungs in RIPA buffer (Sigma) from homogenizer, and then separated on 4–12% NuPAGE gels (Invitrogen). Proteins were then transferred onto Immobilon-P transfer membrane (Millipore Corp.). Membranes were probed with antibodies to *TβRII* (Abcam) and analyzed with the ECL Western blot analysis system as described by the manufacturer (GE Health, Memphis, TN).

In Situ Hybridization—Whole mount and section *in situ* hybridization were performed as previously described (27, 28). The digoxigenin-labeled RNA antisense and sense probes were prepared from following cDNA templates: a 0.4-kb fragment of *SpC*, a 1.4-kb fragment of *Nkx2.1* (29), a 0.5-kb fragment of *Foxj1*, a 0.6-kb fragment of *Shh* (Dr. Andrew P. McMahon, Harvard University), a 0.7-kb fragment of *Ptc* (Dr. Matthew P. Scott, Stanford University), a 0.7-kb fragment of *Gli-1*, a 0.7-kb fragment of *Foxf1* (Dr. Peter Carlsson, Göteborg University), a 0.4-kb fragment of *Fgf10*, a 1.3-kb fragment of *Tbx4*, and a 1-kb fragment of *Tbx5*(Dr. Virginia Papaioannou, Princeton University).

RNA Extraction, Polymerase Chain Reaction (PCR), and Northern Blotting—Total RNA was isolated from embryonic lungs and MRC5 cells (ATCC) by using TRIzol (Invitrogen). Superscript First-Strand Synthesis System kit (Invitrogen) was used to generate cDNA. Quantification of the selected genes by real-time PCR was performed using a LightCycler (Roche Applied Sciences) as previously described (30). Sequence of the primers were as follows: Mouse *TβrII*: 5′-ATG CAT CCA TCC ACG TAA G-3′(forward), 5′-GAC ACG GTA GCA GTA GAA GA-3′ (reverse); human *TβrII*: 5′-CAC GTT CAG AAG TCG GAT GT-3′(forward), 5′-CAT CAG AGC TAC AGG AAC AC-3′(reverse); Mouse *TβrII*(qPCR): 5′-CAT GAA AGA CAG TGT GCT GAG A-3′(forward), 5′-CTC ACA CAC GAT CTG GAT GC-3′(reverse); Mouse *Foxf1*: 5′-AGC ATC TCC ACG CAC TCC-3′(forward), 5′-TGT GAG TGA TAC CGA GGG ATG-3′(reverse); Mouse *Tbx4*: 5′-GCA TGA GAA GGA GCT GTG G-3′(forward), 5′-TTA CCT TGT AGC TGG GGA ACA-3′(reverse); Human *PAI-1*: 5′-AAC GGC CAG TGG AAG ACT C-3′(forward), 5′-GGG CGT GGT GAA CTC AGT AT-3′(reverse); Human *Ptc*: 5′-AAC AAA AAT TCA ACC AAA CCT C-3′(forward), 5′-TGT CCT CGT TCC AGT TGA TGT G-3′(reverse); Human *Gli-1*: 5′-CAG GGA GGA AAG CAG ACT GA-3′(forward), 5′-ACT GCT GCA GGA TGA CTG G-3′(reverse); Human *Fgf10*: 5′-CGG GAC CAA GAA GGA GAA CT-3′(forward), 5′-ACG GCA ACA ACT CCG ATT-3′(reverse); Human *GAPDH*: 5′-GAA GGT GAA GGT CGG AGT C-3′(forward), 5′-GAA GAT GGT GAT GGG ATT TC-3′(reverse). Ten micrograms of total RNA were electrophoresed in 1% RNA formaldehyde-agarose gel and blotted. Blots were hybridized with probes specific for *TβRII*, *Shh*, *Ptc*, *Gli-1*, *Fgf10*, *Gapdh*, and then autoradiographed or measured with Kodak Molecular Imaging Software Ver 4.0 to determine the quantity. ^{32}P-labeled probes were synthesized from the following cDNA fragments: the *TβRII* probe was from a 0.4-kb PCR product of *TβRII* coding region. The *Shh* probe was from a 0.6-kb cDNA (Dr. Brigid L. M. Hogan, Vanderbilt University). The *Ptc* probe was from a 0.7-kb cDNA (Dr. Matthew P. Scott, Stanford University), The *Gli-1* probe was from a 0.7-kb cDNA. The *Fgf10* probe was from a 0.4-kb cDNA. The *GAPDH* probe was as reported before (31).

Cell Culture and TGF-β Treatment—Human pulmonary mesenchymal cell line MRC5 (ATCC, Manassas, VA) was maintained in EMEM medium (ATCC), containing 10% fetal

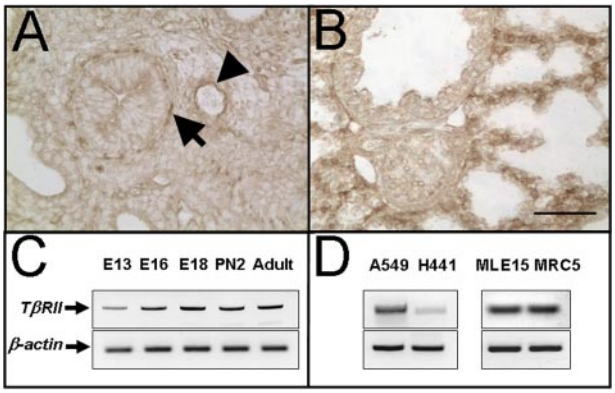

FIGURE 1. **TβRII expression in the murine lung.** *A* and *B* show immunolocalization of TβRII protein in lungs from E15.5 and E18.5 embryos, respectively. The *arrow* shows TβRII protein localized in the subepithelial layer of proximal airways. The *arrowhead* points to endothelial localized TβRII around the blood vessel. *B* shows immunolocalized TβRII distributed throughout the parenchyma of E18.5 lungs, with highest expression in the interstitium, including cells of mesenchymal origin. *C*, semi-quantitative RT-PCR of *TβRII* mRNA during murine lung morphogenesis. *E*, embryonic day; *PN*, postnatal day. *D*, *TβRII* mRNA is also detectable in both human (A549 and H449) and murine (MLE15) transformed epithelial cell lines. MRC5 is a fetal human mesenchymal cell line. *Scale bar*, 100 μm.

bovine serum and 1% penicillin-streptomycin. MRC5 cells were treated with recombinant TGF-β (R&D systems, Minneapolis, MN) at 200 ng/ml for 2 h and then collected for RNA extraction.

RESULTS

TβRII Expression during Lung Development—TβRII has been reported to be expressed in both the epithelium and the mesenchyme of the lung (32). To elucidate the expression pattern of *TβRII* in the murine lung, we used semi-quantitative RT-PCR and immunohistochemistry. Expression of *TβRII* mRNA can be detected by RT-PCR throughout lung development (Fig. 1 *C*). Commercially available antibody (Abcam) detects TβRII protein in mesenchymal cells localized around the airways (Fig. 1, *arrows*) and blood vessels (Fig. 1, *arrowhead*) in E15.5 lungs (Fig. 1*A*) and throughout the mesenchyme in E18 lungs (Fig. 1*B*). *TβRII* mRNA is clearly expressed in human lung epithelial carcinoma, H441 and A549 cell lines as well as mouse-immortalized epithelial MLE15 cells (Fig. 1*D*).

Recombination Mediated by Dermo1-cre in the Lung Mesenchyme—Recombination driven by *Dermo1-cre* in the lung was analyzed by crossing with the reporter mouse strain *Rosa26-LacZ*. Double transgenic, *Rosa26-LacZ; Dermo1-cre* fetuses were identified by PCR genotyping, and the lungs were excised and stained for LacZ. As shown in Fig. 2*A*, expression of *Dermo1-cre* resulted in nearly 100% recombination of the *loxP* sites in *Rosa26-lacZ* lung mesodermal cells (Fig. 2*A*, *panels a–f*). This recombination was entirely mesenchymal-specific in that no epithelial cells showed LacZ staining (Fig. 2*A*, *panels a*, *b*, *d*, and *f*, *arrows*).

Inactivation of TβRII by Dermo1-cre-driven Recombination—Conventional deletion of *TβRII* led to early embryonic lethality (22). Thus, we used a conditional Cre-LoxP approach to specifically delete exon 2 in the *TβRII* locus in mesodermal lineages, including those of the lung. Accordingly, we crossed $T\beta RII^{fl/fl}$ females with *Dermo1-cre* male mice and backcrossed the heterozygotes to generate $T\beta RII^{fl/fl}$*; Dermo1-cre* progeny. The latter genotype is referred to simply as $T\beta RII^{\Delta/\Delta}$. To validate Dermo1-cre-induced recombination and deletion of exon 2 within the *TβRII* gene, we used three approaches. First, we utilized lung DNA with PCR primers that could distinguish between deleted and intact *TβRII* alleles. The deletion in *TβRII* gene was verified by genomic PCR analysis shown in Fig. 2*B*, *panel b*. Second, we measured TβRII protein content by Western blot analysis in protein extracts of total lung tissue from control and $T\beta RII^{\Delta/\Delta}$ embryos. These studies showed greater than 60% decrease in total lung TβRII protein, the remainder indicating non-mesenchymal (*e.g.* epithelial and endothelial) TβRII protein (Fig. 2*B*, *panels c* and *d*). In contrast, the protein level of TβRI and phosphorylated Smad2 (p-Smad2) remained the same. Therefore mesenchymal deletion of *TβRII* in the lung does not alter the level of phosphorylated Smad2 and TβRI. Finally, functional deletion of *TβRII* was verified by immunohistochemistry using antibodies to Plasminogen Activator Inhibitor (PAI-1), which is a downstream target of TGF-β signaling. In the control lungs, diffuse PAI-1 was detected throughout both the epithelium and the mesenchyme, but particularly in the progenitor of parabronchial smooth muscle cells (PBSMC) in the subepithelial mesoderm (Fig. 2*C*, *panel b*, *arrows*). In contrast, PAI-1 in the $T\beta RII^{\Delta/\Delta}$ lungs was found only in the epithelium. As expected, there was virtually no PAI-1 staining in the mesoderm, nor in the PBSMC progenitors in $T\beta RII^{\Delta/\Delta}$ lungs (Fig. 2*C*, *panel d*, *arrowheads*).

Ultrastructure and Cellular Differentiation in $T\beta RII^{\Delta/\Delta}$ *Lungs*—Dermo1-cre-induced deletion of exon 2 within the *TβRII* gene was embryonically lethal by day 16–17 of gestation. E16–17 fetuses developed gross abnormalities in multiple organs that caused fetal demise. We therefore, collected and characterized lungs from $T\beta RII^{\Delta/\Delta}$ E15.5 fetuses. Gross morphological assessment of the proximal lung structure showed a readily discernible phenotype manifested as disorganized formation of tracheal cartilage (Fig. 3*N*). Both the number as well as the shape of the tracheal cartilage was altered. The first and the second generation bronchi in the mutant lungs were devoid of cartilage altogether (not shown).

Mesodermal deletion of *TβRII* also impacted the shape and the size of the various lung lobes as shown in Fig. 3. However, the overall process of lobation and the number of lobes were normal (Fig. 3, *H–L*). Histological assessment showed a distinct phenotype in $T\beta RII^{\Delta/\Delta}$ lungs, characterized by the presence of large, dilated airways, lined with columnar epithelial cells in the proximal lung (Fig. 4*A*).

The epithelial cells throughout the $T\beta RII^{\Delta/\Delta}$ lungs showed expression of NKX2.1, a transcription factor associated with onset of lung epithelial morphogenesis and normal lung structural development(Fig. 4*B*, *panels a* and *d*) (33). Transcripts for Surfactant Protein C, SPC, a marker of distal epithelial cells and a target of NKX2.1 was also expressed in the mutant lungs. Also, differentiation of ciliated cells as evidenced by expression of *Foxj1* appeared to be normal in the absence of epithelial *TβRII* activity (Fig. 4*B*). The normal level and distribution of Surfactant Protein B, SPB, expressed in proximal and distal, differentiated epithelium, as well as β-tubulin, an established marker of airway ciliated cells were also observed by immunohistochem-

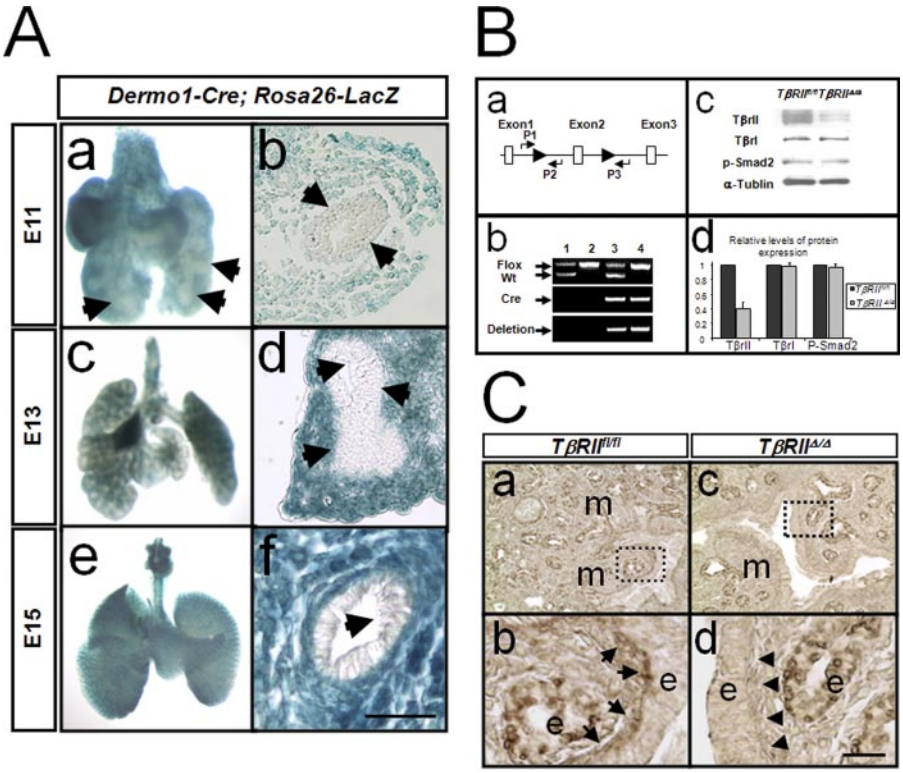

FIGURE 2. **Generation and validation of *TβRII* conditional knock-out alleles.** *A*, mesenchymal specific recombination induced by *Dermo1-cre* as determined by LacZ assay in murine lungs from various stages of embryonic development. *Panels a*, *c*, and *e* are whole mount lung tissue. *Panels b*, *d*, and *f* are frozen saggital sections of the lungs in *panels a*, *c*, and *e*. *Arrows* in *panels a*, *b*, *d*, and *f* show the absence of LacZ in airway epithelial cells. *Scale bar*, 50 μm. *B*, evidence for deletion of *TβRII* gene by *Dermo1-cre*. *Panel a*, map of the mouse *TβRII* locus showing the relative position of the lox-P (flox) sequences and the primers used in identifying various genotypes. Primers for Cre were used as described by Yu *et al.* (23). *Panel b*, PCR analysis of *TβRII* gene using lung-extracted DNA and the primers P1, P2, and P3, as shown in *panel a*. *Lane 1*, $T\beta RII^{fl/+}$ lungs, showing two bands corresponding to the wild type (*Wt*) and the allele carrying the lox-P insertion. The absence of a PCR product using P1/P3 primers is due to the large distance between the two primers (absence of deletion). *Lane 2*, $T\beta RII^{fl/fl}$ lungs showing a single band corresponding to floxed allele. *Lane 3*, $T\beta RII^{\Delta/+}$ lungs. Deletion of Exon 2 brings the sequences recognized by P1 and P3 primers sufficiently close to allow amplification of a PCR product (deletion). *Lane 4*, $T\beta RII^{\Delta/\Delta}$ lungs. *Panel c*, Western blot analysis of TβRII, TβRI, and p-Smad2 in total lung protein from $T\beta RII^{fl/fl}$ (*lane 1*) and $T\beta RII^{\Delta/\Delta}$ (*lane 2*) mice. *Panel d*, densitometric quantification of the Western blot shown in *panel c*. *C*, immunohistochemical analysis for PAI-1 in $T\beta RII^{\Delta/\Delta}$ and $T\beta RII^{fl/fl}$ lungs. *Arrowheads* in *panel d* show the reduced expression of PAI-1 in the PBSMCs of mutant lungs compared with *arrows* in *panel b* (control). *m*, mesenchyme; *e*, epithelium. *Scale bar*, 100 μm for *panels a* and *c*, 23 μm for *panels b* and *d*.

istry (data not show). Collectively, these data indicate that the absence of *TβRII* in the lung mesenchyme does not alter lung epithelial cell identity and differentiation.

Expression of TGF-β Targets in $T\beta RII^{\Delta/\Delta}$ Lungs—In wild-type embryonic lungs, α-smooth muscle actin-positive cells are found as rings of smooth muscle progenitor cells surrounding the columnar epithelium of the proximal airways (Fig. 4*C*, *panel a*). In contrast, we found reduced α-SMA-positive cells surrounding the dilated airways in the mutant lungs (Fig. 4*C*, *panel b*). This is the same layer of smooth muscle cells in which PAI-1 was found to be abundantly expressed in the wild-type lung and drastically reduced in $T\beta RII^{\Delta/\Delta}$ lungs (Fig. 2*C*). Immunohistochemistry was also performed to determine potential changes in the expression or spatial localization of other mesenchymal genes including collagen type I and platelet/endothelial cell adhesion molecule (PECAM) known to be modulated by TGF-β (6, 34). Reduced levels of PECAM were found in the mutant lungs (Fig. 4*C*, compare *panels c* and *d*). Another marker of endothelial cell differentiation, Flk1 appeared to have the same level and distribution in the mutant lungs as wild type (Fig. 4*C*, *panels e* and *f*). Collagen production is also under TGF-β control (6). Both in the wild-type control and the mutant lungs, collagen Type I was localized to the extracellular matrix surrounding both the distal and the proximal airways (Fig. 4*C*, *panels g* and *h*). No drastic alteration in collagen type I was observed in $T\beta RII^{\Delta/\Delta}$ lungs suggesting that either TGF-β is signaling through utilization of type I receptor (homotetramer) or that collagen production and deposition may not be entirely TGF-β-dependent.

Expression of Fgf10 in $T\beta RII^{\Delta/\Delta}$ Lungs—Whole mount and section *in situ* hybridization were performed for a number of genes with established roles during lung morphogenesis. Because the shape and size of the airways can be regulated by FGF10 activity and its expression domain, we investigated the expression pattern of *Fgf10* in $T\beta RII^{\Delta/\Delta}$ lungs. Whole mount *in situ* hybridization revealed increased expression, and expansion of the *Fgf10* domain in the mutant embryonic lungs (Fig. 5*A*, *panels e* and *f*). A clearer demonstration of this alteration was observed by *in situ* hybridization experiments on tissue sections (Figure 5*A*, compare *panels c* and *g*). In the control lungs, *Fgf10* mRNA was localized to mesenchymal cells adjacent to the growing tip of the peripheral airways (Fig. 5*A*, *panels c* and *d*) consistent with previously reported results (12). In the mutant lungs, however, we found an expanded *Fgf10* expression domain and likely increased mRNA in the peripheral mesenchyme adjacent to the branching airways (Fig. 5*A*, *panels e–h*). This alteration in *Fgf10* expression domain may explain the phenotype of the $T\beta RII^{\Delta/\Delta}$ lungs in which airways are significantly dilated. Two transcription factors, Foxf1 and Tbx4 have been found to stimulate *Fgf10* expression in the lung mesenchyme (35, 36). Consistent with this finding, *in situ* hybridization on tissue sections (Fig. 5*B*, *panels a*, *b*, *d*, and *e*) and real-time PCR (Fig. 5*C*) revealed increased transcripts for both in $T\beta RII^{\Delta/\Delta}$ lungs compared with controls. Expression of another *Tbx* gene, *Tbx5* remained unchanged (Fig. 5*B*, *panels c* and *f*). These data support the finding that *Fgf10* is both increased and expanded in its expression domain in $T\beta RII^{\Delta/\Delta}$ lungs.

Cross-talk between TGF-β and Shh Pathways—Shh is thought to negatively regulate *Fgf10* magnitude and distribution, thereby, controlling lung branching morphogenesis (20,

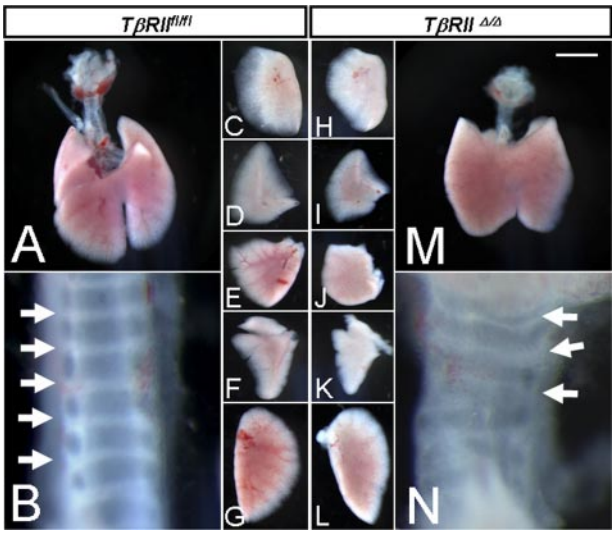

FIGURE 3. **Gross morphology of $T\beta RII^{\Delta/\Delta}$ and $T\beta RII^{fl/fl}$ trachea and lungs from E15.5 embryos.** *B* and *N*, tracheas. *Arrows* show abnormal number and shape of tracheal cartilage. *C* and *H*, right apical lobes. *D* and *I*, right middle lobes. *E* and *J*, right caudal lobes. *F* and *K*, accessory lobes. *G* and *L*, left lobes. *Scale bar*, 1.0 mm for *A* and *M*; 0.2 mm for *B* and *N*; 0.8 mm for *C–F*, *H–K*, and 1.2 mm for *G* and *L*.

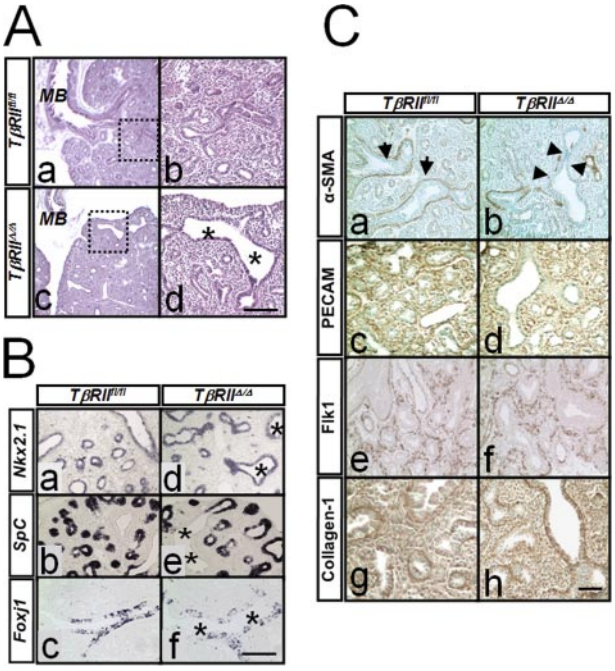

FIGURE 4. **H & E staining and immunohistochemical analysis for lung developmental markers in $T\beta RII^{\Delta/\Delta}$ and control lungs.** *A*, gross histology of lungs from $T\beta RII^{fl/fl}$ (*panels a* and *b*) and $T\beta RII^{\Delta/\Delta}$ (*panels c* and *d*) E15.5 embryos. Saggital sections of lungs were analyzed by H & E staining. *MB*, mainstem bronchus. *Asterisks* show dilated proximal airways. *Panels b* and *d* are high magnification of areas within *dotted squares* in *panels a* and *c*, respectively. *Scale bar*, 330 μm for *panels a* and *c*; 100 μm for *panels b* and *d*. *B*, cell differentiation in $T\beta RII^{\Delta/\Delta}$ embryonic lungs. *In situ* hybridization for *Nkx2.1* (*panels a* and *d*), *SpC* (*panels b* and *e*), and *Foxj1* (*panels c* and *f*). *Asterisks*, dilated airways. *Scale bar*, 100 μm. *C*, immunohistochemical analysis for α-SMA (*panels a* and *b*), PECAM (*panels c* and *d*), Flk1 (*panels e* and *f*), and Collagen1 (*panels g* and *h*) in E15.5 $T\beta RII^{fl/fl}$ and $T\beta RII^{\Delta/\Delta}$ lungs. *Arrowheads* in *panel b* show reduced expression of α-SMA surrounding the dilated airways of mutant lungs compared with *arrows* in *panel a* (control). *Scale bar*, 100 μm.

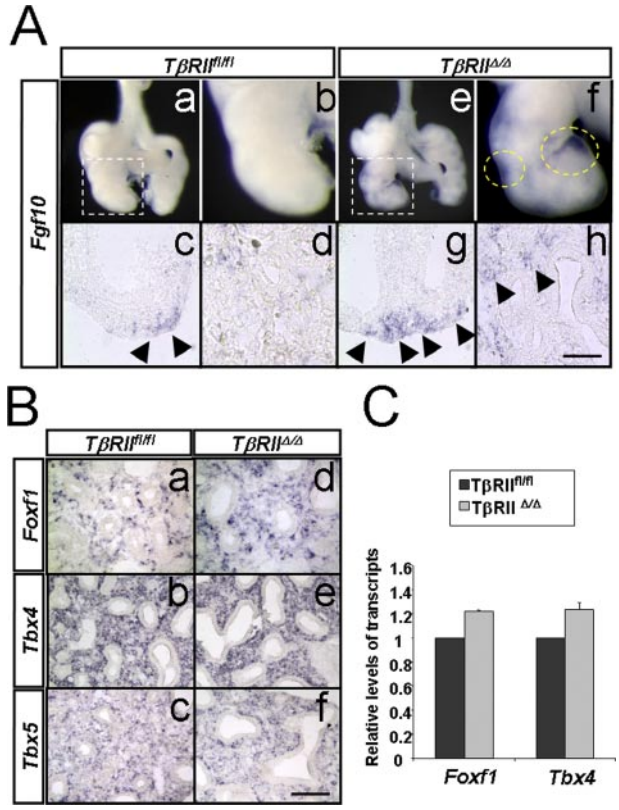

FIGURE 5. ***In situ* hybridization analysis of Fgf10 and its upstream transcriptional regulators in $T\beta RII^{\Delta/\Delta}$ and control lungs.** *A*, whole mount (*panels a*, *b*, *e*, and *f*) and section (*panels c*, *d*, *g*, and *h*) *in situ* hybridization. Note expansion and increased *Fgf10* expression in $T\beta RII^{\Delta/\Delta}$ (*panels e–h*) compared with $T\beta RII^{fl/fl}$ (*panels a–d*) lungs. *Scale bar*, 2.2 mm (*panels a* and *c*); 1 mm (*panels b* and *d*); 100 μm (*panels e–h*). *B*, section *in situ* hybridization for *Foxf1* (*panels a* and *d*), *Tbx5* (*panels b* and *e*), and *Tbx4* (*panels c* and *f*) in $T\beta RII^{\Delta/\Delta}$ and $T\beta RII^{fl/fl}$ (control) E15.5 lungs. *Scale bar*, 100 μm. *C*, quantification of *Foxf1* and *Tbx4* mRNA by real-time PCR. Values are fold induction or repression, compared with $T\beta RII^{fl/fl}$ controls (arbitrarily adjusted to 1). *p* value, 0.004.

37). The mechanistic connection between *Fgf10* and Shh remained unknown. We therefore examined Shh signaling by investigating the level and distribution of *Shh* and its downstream targets *Ptc* and *Gli-1* in the mutant lungs compared with the $T\beta RII^{fl/fl}$ controls. Whole mount and tissue section *in situ* hybridization showed similar levels and spatial localization of *Shh* mRNA in the control and mutant lungs (Fig. 6, *A*, *D*, *G*, and *J*). In contrast, there was a significant increase in the level of mRNA for both *Ptc* (Fig. 6, *B*, *E*, *H*, and *K*) and *Gli-1* (*C*, *F*, *I*, and *L*) in the $T\beta RII^{\Delta/\Delta}$ mutant lungs compared with the control. To validate the above *in situ* hybridization results, we used Northern blot analysis as shown in Fig. 7. Transcripts for *TβRII* were decreased by nearly 80% in $T\beta RII^{\Delta/\Delta}$ lung tissue, compared with controls. Other changes included a ~1.8-fold increase in *Ptc* and *Gli-1* mRNA and a 1.5-fold increase in *Fgf10*. The magnitude of *Shh* remained nearly the same in the mutant and control lungs confirming the *in situ* hybridization findings.

Because deletion of *TβRII* occurs specifically in the lung mesenchyme, one potential hypothesis is that TGF-β signaling through *TβRII* normally represses *Gli-1* and *Ptc* mRNA levels in the lung mesenchymal cell layer. To determine the validity of this hypothesis, we used cultured MRC5 cells, which are derived from normal lung mesenchymal cells of a 14-week-old male fetus, and assessed the impact of exogenous TGF-β treatment on *Gli-1* and *Ptc* mRNA levels by real-time PCR. In support of our *in vivo* observations, the results clearly showed that TGF-β represses steady state levels of both *Gli-1* and *Ptc*

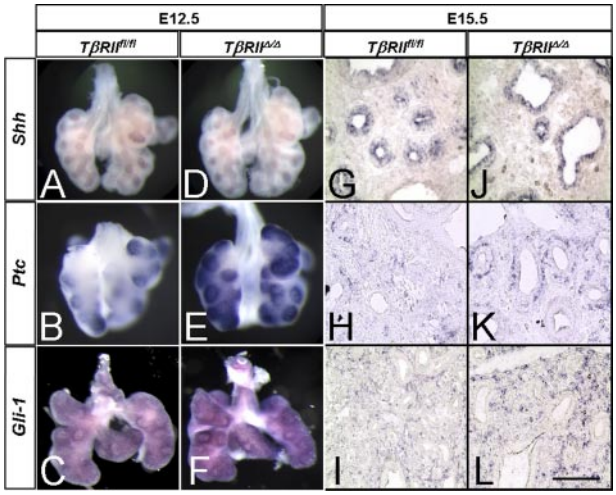

FIGURE 6. **Whole mount and section *in situ* hybridization for components of the Shh pathway in *TβRII*$^{fl/fl}$ and *TβRII*$^{Δ/Δ}$ E12.5 (*A–F*) and E15.5 (*G–L*) lungs.** Abundance of mRNA for both *Ptc* and *Gli-1* is increased in the mutant lungs (*E*, *F*, *K*, and *L*) compared with the control lungs (*B*, *C*, *H*, and *I*). Little if any change is detectable in the epithelial-localized *Shh* (*A*, *D*, *G*, and *J*). *Scale bar*, 2.2 mm (*A*, *B*, *E*, *F*, *I*, *J*); 100 μm (*C*, *D*, *G*, *H*, *K*, *L*).

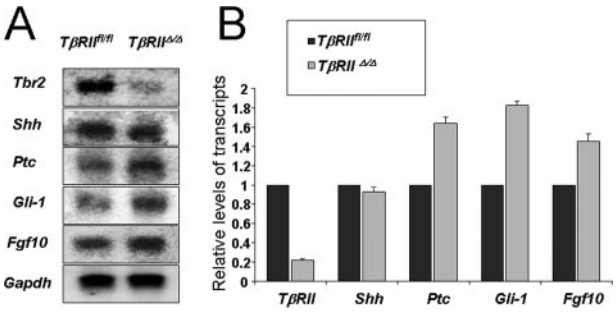

FIGURE 7. **Quantification of mRNA changes in *TβRII*$^{Δ/Δ}$ lungs.** Total RNA from E15.5 *TβRII*$^{Δ/Δ}$ and *TβRII*$^{fl/fl}$ (control) embryonic lungs was used for Northern blot analysis (*A*), and the results were quantified by densitometry and normalized by GAPDH (*B*). Values are fold induction or repression, compared with *TβRII*$^{fl/fl}$ controls (arbitrarily adjusted to 1).

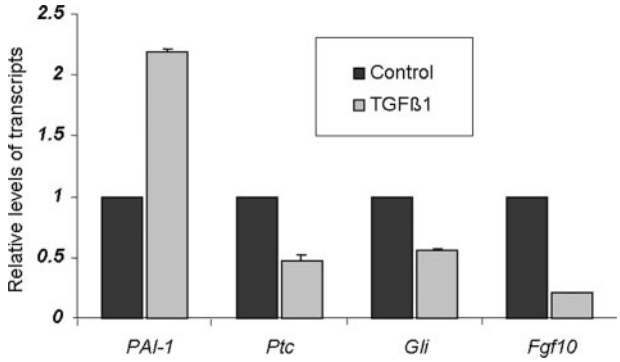

FIGURE 8. ***In vitro* verification of the *in vivo* evidence that TGF-β is a negative regulator of Shh pathway.** MRC5 cells were treated with either 200 ng/ml of TGF-β1 or equivalent bovine serum albumin (control). Real-time PCR-quantified mRNA for *PAI-1* (positive control), *Ptc* and *Gli-1*. Values are fold induction or repression, compared with controls (adjusted to 1).

mRNAs by nearly 50% (Fig. 8). *Fgf10* has been proposed to be a target of Shh signaling in the lung (36) although this regulation has not been experimentally explored or demonstrated. In MRC5 cells, TGF-β treatment repressed *Fgf10* mRNA consistent with our *in vivo* observations in Fig. 5*A*. Thus, these *in vitro* results validate our *in vivo*-based conclusions and support a model for interactions between TGF-β and Shh signaling pathways (Fig. 9).

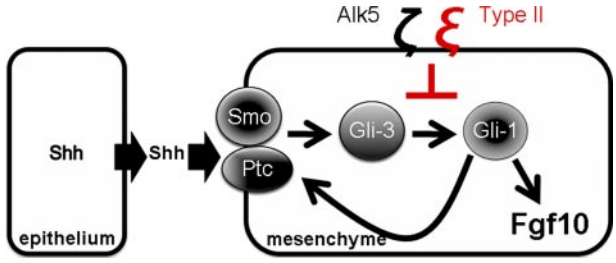

FIGURE 9. **A hypothetical model for TGF-β~Shh cross-talk in the developing lung.** Shh is made in the lung epithelium. The Shh receptor complex, Ptc/smoothened is expressed on the cell surface of lung mesenchymal cells. Activation of Shh pathway leads to increased Gli-3 activity, which in turn stimulates *Gli-1* and *Ptc* transcription. TGF-β ligand acts through TβRII and as yet unknown intracellular mediators (*e.g.* Smads) to interfere with Shh signal transduction in mesenchymal cells, evidenced by reductions in both *Ptc* and *Gli-1* observed in this study.

DISCUSSION

The purpose of the current study was to examine the consequences of interruption in mesenchymal TβRII-mediated TGF-β signaling on lung morphogenesis. To this end, we generated mice carrying mesodermal-specific deletion of the *TβRII* exon 3 by Dermo1-cre-driven recombination. *TβRII*$^{Δ/Δ}$ fetuses died *in utero* due to multi-organ abnormalities. Examination of embryonic lungs revealed that mesenchymal abrogation of endogenous TGF-β signaling caused abnormalities in epithelial morphogenesis, indicating disruption of normal epithelial-mesenchymal communication that is central to lung development. Analysis of key mediators of this cross-talk showed alterations in components of the Shh pathway. Both *Ptc* and *Gli-1* as well as the transcription factor *Foxf1* were increased in the mesenchyme of the mutant lungs. *Shh* mRNA in the lung epithelium was unchanged. Thus, abrogation of TβRII-mediated signaling in the lung mesenchyme results in increased expression of *Shh* downstream targets (*i.e.* Shh signaling). To our knowledge, this is the first demonstration of cross-communication between the TGF-β and the Shh pathways during vertebrate embryonic development.

At least two major phenotypic abnormalities were readily observable in *TβRII* mutant lungs. First, the trachea of the mutant lungs showed abnormalities in both structure and number of cartilage. Both TGF-β and Shh are known to be involved in the induction of early cartilaginous differentiation of mesenchymal cells in the limb and in the spine. *In vitro*, treatment of human bone marrow-derived mesenchymal stem cells (MSCs) with either TGF-β or recombinant Shh induced expression of cartilage markers aggrecan, Sox9, CEP-68, and collagen type II and X (38). Thus, the abnormalities observed in tracheal cartilage formation in *TβRII*$^{Δ/Δ}$ lungs can be explained as either a direct result of mesenchymal *TβRII* deletion or indirect effect of interruption in Shh signaling.

Mesodermal inactivation of *TβRII* also caused abnormal epithelial morphogenesis manifested as cystic, dilated bronchi (Figure 4*A*). Lung branching morphogenesis is strictly dependent on epithelial-mesenchymal communication between the

foregut endoderm and the mesodermal-derived splanchnic mesenchyme. The lung mesenchyme, via Fgf10 provides instructional signaling that directs epithelial morphogenesis. Targeted deletion of *Fgf10* results in profoundly abnormal lungs that lack structures distal to the main stem bronchi (13, 14). Dynamic changes in the magnitude and spatial distribution of *Fgf10* are critical to normal branching morphogenesis and are thought to be controlled by diffusible signals originating from the epithelial cells themselves. Shh is expressed in the distal epithelium, from where it activates signaling in the corresponding mesenchyme via its receptor, the patched (Ptch1)/smoothened (Smo) complex and their transcriptional effectors Gli-1, Gli-2, and Gli-3 (9, 11). Results from both *in vitro* and *in vivo* studies indicate that Shh negatively regulates Fgf10 production in the lung mesenchyme (20, 37). Thus, a current model of embryonic lung development is centered on epithelial Shh as playing a dual role in both activating and limiting mesenchymal signaling thereby "fine-tuning" the process of branching morphogenesis. In *Shh*(−/−) lungs, *Fgf10* mRNA is found diffusely throughout the mesenchyme, as a consequence of which the airways develop into large cystic structures and branching morphogenesis is severely disrupted (20). Although not as severe, the phenotypically abnormal, cystic bronchi observed in *TβRII* mutant lungs are similar to those observed in *Shh*(−/−) lungs (Fig. 4*A*). *In situ* hybridization revealed a clear expansion of the *Fgf10* domain in E15.5 $T\beta RII^{\Delta/\Delta}$ lungs (Fig. 5*A*). Consistent with these results, *Foxf1* and *Tbx4*, two transcription factors that stimulate *Fgf10* production in the lung mesenchyme (35, 36), were also increased in the $T\beta RII^{\Delta/\Delta}$ lungs (Fig. 5, *B* and *C*).

An abnormal characteristic of the cystic bronchial airways in *TβRII* lungs was the absence of PBSMCs (Fig. 4*C*). During development and in adult tissues, mesenchymal cells serve as precursors to diverse cell lineages, including PBSMCs. The function of TGF-β in promoting myofibroblast differentiation is well recognized (39, 40). Therefore, the absence of PBSMCs may be a direct impact of mesenchymal *TβRII* inactivation, suggesting that TGF-β signaling via the Type II receptor is required for PBSMC differentiation. The relatively high level of endogenous TβRII protein and the TGF-β target, PAI-1 in the PBSMCs (Figs. 1 and 2*C*) and drastic reduction of PAI-1 in response to mesodermal deletion of *TβRII* in these cells in the mutant lungs (Fig. 2*C*, *panel d*) supports the above hypothesis. In addition however, we showed previously that PBSMC progenitors express *Fgf10*, and the transcription factor *Pitx2,* both of which may be important in maintaining their undifferentiated status (41). These proliferating cells cease to express *Fgf10* before onset of differentiation into PBSMCs (42). Thus, increased levels, or spatial expansion of *Fgf10* distribution in *TβRII* mutants, may provide another, alternative mechanistic explanation for the absence of PBSMCs in the dilated bronchial airways; high levels of *Fgf10* may inhibit PBSMC differentiation.

TGF-β signaling is inhibitory to branching morphogenesis (21). Activation of TGF-β in mesenchymal cells markedly inhibits *Fgf10* expression (37, 43, 44). Positive transcriptional regulators of *Fgf10, Tbx4*, and *Foxf1* are controlled by Shh signaling that emanates from the branching epithelium. Recently, potential interactions between Shh and TGF-β pathways have been examined in *in vitro* settings. Shh promotes motility and invasiveness of gastric cancer cells through TGF-β-mediated activation of the ALK5-Smad3 pathway (45). In contrast to our findings, TGF-β was shown to induce *Gli-1* and *Gli-2* expression in various human cell lines (46). Also, in transgenic mice overexpressing TGF-β1 in the skin, *Gli-1* and *Gli-2* were elevated in a Smad3-dependent manner (46). This apparent discrepancy may suggest both cell type (skin *versus* lung) and dose-dependent specificity of TGF-β effect on adult and embryonic tissue. The relationship between TGF-β and Shh during organogenesis, the focus of the present study had remained unknown. In particular whether the inhibition of *Fgf10* in the lung mesenchyme in response to TGF-β involves the Shh pathway remained unknown. We found increased expression of *Ptc* and *Gli-1*, as well as the transcription factors *Tbx4* and *Foxf1* in the mesenchyme of *TβRII* mutant lungs, suggesting that endogenous TGF-β signaling via the type II receptor in the wild-type lung regulates Shh signal transduction in the mesenchyme. In previous studies, we found that Wnt5a alters Shh signaling by modulating *Shh* mRNA in the lung epithelium (30). In contrast, increased Shh signaling in the mesenchyme in response to TβRII inactivation occurrs in the absence of changes in epithelial *Shh* mRNA (Figs. 6 and 7). Therefore, TGF-β does not directly interfere with Shh originating from the lung epithelium, but dampens its transduction within the target tissue, the lung mesenchyme. This interference by TGF-β may provide a potential mechanism by which Shh limits *Fgf10* expression domain in the lung mesenchyme during branching morphogenesis. *In vitro* studies using MRC5 cells, showed that treatment with TGF-β reduces the steady state level of *Fgf10*, concomitant with decreases in *Ptc* and *Gli-1* mRNAs (Fig. 8) thereby validating the *in vivo* observations. Based on the collective *in vivo* and *in vitro* findings, a hypothetical model depicting the mechanisms of TGF-β∼Shh cross-talk is proposed in Fig. 9. In the wild-type lung, TGF-β fine-tunes Shh signaling through modulation of its downstream targets, *Gli-1* and *Ptc*, which in turn may control the magnitude and spatial distribution *Fgf10*. In this manner, TGF-β signaling via TβRII participates in the response of mesenchymal cells to Shh signaling that originates from the lung epithelium.

Acknowledgments—We thank Dr. Yang Chai for providing the homozygous TβRII mutant mice, Dr. Andrew P. McMahon for Shh cDNA, Dr. Matthew P. Scott for Ptc cDNA, Dr. Peter Carlsson for Foxf1 cDNA, and Dr. Virginia Papaioannou for Tbx4 and Tbx5 cDNA.

REFERENCES

1. Massague, J. (1998) *Annu. Rev. Biochem.* **67,** 753–791
2. Souchelnytskyi, S., Tamaki, K., Engstrom, U., Wernstedt, C., ten Dijke, P., and Heldin, C. H. (1997) *J. Biol. Chem.* **272,** 28107–28115
3. Wrana, J. L. (2000) *Sci STKE* 2000, **2000,** RE1
4. Sanford, L. P., Ormsby, I., Gittenberger-de Groot, A. C., Sariola, H., Friedman, R., Boivin, G. P., Cardell, E. L., and Doetschman, T. (1997) *Development* **124,** 2659–2670
5. Kaartinen, V., Voncken, J. W., Shuler, C., Warburton, D., Bu, D., Heisterkamp, N., and Groffen, J. (1995) *Nat. Genet.* **11,** 415–421
6. Zhou, L., Dey, C. R., Wert, S. E., and Whitsett, J. A. (1996) *Dev. Biol.* **175,** 227–238

7. Chen, H., Sun, J., Buckley, S., Chen, C., Warburton, D., Wang, X. F., and Shi, W. (2005) *Am. J. Physiol. Lung Cell Mol. Physiol.* **288,** L683–L691
8. Shannon, J. M., and Hyatt, B. A. (2004) *Annu. Rev. Physiol.* **66,** 625–645
9. Tabin, C. J., and McMahon, A. P. (1997) *Trends Cell Biol.* **7,** 442–446
10. Miller, L. A., Wert, S. E., and Whitsett, J. A. (2001) *J. Histochem. Cytochem.* **49,** 1593–1604
11. Bellusci, S., Furuta, Y., Rush, M. G., Henderson, R., Winnier, G., and Hogan, B. L. (1997) *Development* **124,** 53–63
12. Bellusci, S., Grindley, J., Emoto, H., Itoh, N., and Hogan, B. L. (1997) *Development* **124,** 4867–4878
13. Sekine, K., Ohuchi, H., Fujiwara, M., Yamasaki, M., Yoshizawa, T., Sato, T., Yagishita, N., Matsui, D., Koga, Y., Itoh, N., and Kato, S. (1999) *Nat. Genet.* **21,** 138–141
14. Min, H., Danilenko, D. M., Scully, S. A., Bolon, B., Ring, B. D., Tarpley, J. E., DeRose, M., and Simonet, W. S. (1998) *Genes Dev.* **12,** 3156–3161
15. Ingham, P. W. (1995) *Curr. Opin. Genet. Dev.* **5,** 492–498
16. McMahon, A. P. (2000) *Cell* **100,** 185–188
17. Dai, P., Akimaru, H., Tanaka, Y., Maekawa, T., Nakafuku, M., and Ishii, S. (1999) *J. Biol. Chem.* **274,** 8143–8152
18. Grindley, J. C., Bellusci, S., Perkins, D., and Hogan, B. L. (1997) *Dev. Biol.* **188,** 337–348
19. Motoyama, J., Liu, J., Mo, R., Ding, Q., Post, M., and Hui, C. C. (1998) *Nat. Genet.* **20,** 54–57
20. Pepicelli, C. V., Lewis, P. M., and McMahon, A. P. (1998) *Curr. Biol.* **8,** 1083–1086
21. Xing, Y., Li, C., Hu, L., Tiozzo, C., Li, M., Chai, Y., Bellusci, S., Anderson, S., and Minoo, P. (2008) *Dev. Biol.* **320,** 340–350
22. Oshima, M., Oshima, H., and Taketo, M. M. (1996) *Dev. Biol.* **179,** 297–302
23. Yu, K., Xu, J., Liu, Z., Sosic, D., Shao, J., Olson, E. N., Towler, D. A., and Ornitz, D. M. (2003) *Development* **130,** 3063–3074
24. Soriano, P. (1999) *Nat. Genet.* **21,** 70–71
25. Chytil, A., Magnuson, M. A., Wright, C. V., and Moses, H. L. (2002) *Genesis* **32,** 73–75
26. Pan, Q., Li, C., Xiao, J., Kimura, S., Rubenstein, J., Puelles, L., and Minoo, P. (2004) *Gene* **331,** 73–82
27. Li, C., Xiao, J., Hormi, K., Borok, Z., and Minoo, P. (2002) *Dev. Biol.* **248,** 68–81
28. Li, M., Wu, X., Zhuang, F., Jiang, S., Jiang, M., and Liu, Y. H. (2003) *Dev. Dyn.* **228,** 273–280
29. Minoo, P., Hu, L., Xing, Y., Zhu, N. L., Chen, H., Li, M., Borok, Z., and Li, C. (2007) *Mol. Cell. Biol.* **27,** 2155–2165
30. Li, C., Hu, L., Xiao, J., Chen, H., Li, J. T., Bellusci, S., Delanghe, S., and Minoo, P. (2005) *Dev. Biol.* **287,** 86–97
31. Hamdan, H., Liu, H., Li, C., Jones, C., Lee, M., deLemos, R., and Minoo, P. (1998) *Biochim. Biophys. Acta* **1396,** 336–348
32. Zhao, Y., and Shah, D. U. (2000) *Exp. Mol. Pathol.* **69,** 67–78
33. Minoo, P., Su, G., Drum, H., Bringas, P., and Kimura, S. (1999) *Dev. Biol.* **209,** 60–71
34. Zeng, X., Gray, M., Stahlman, M. T., and Whitsett, J. A. (2001) *Dev. Dyn.* **221,** 289–301
35. del Moral, P. M., De Langhe, S. P., Sala, F. G., Veltmaat, J. M., Tefft, D., Wang, K., Warburton, D., and Bellusci, S. (2006) *Dev. Biol.* **293,** 77–89
36. Cardoso, W. V., and Lu, J. (2006) *Development* **133,** 1611–1624
37. Lebeche, D., Malpel, S., and Cardoso, W. V. (1999) *Mech. Dev.* **86,** 125–136
38. Warzecha, J., Gottig, S., Bruning, C., Lindhorst, E., Arabmothlagh, M., and Kurth, A. (2006) *J. Orthop. Sci.* **11,** 491–496
39. Cohen, P., Rajah, R., Rosenbloom, J., and Herrick, D. J. (2000) *Am. J. Physiol. Lung Cell Mol. Physiol.* **278,** L545–L551
40. Black, P. N., Young, P. G., and Skinner, S. J. (1996) *Am. J. Physiol.* **271,** L910–L917
41. De Langhe, S. P., Carraro, G., Tefft, D., Li, C., Xu, X., Chai, Y., Minoo, P., Hajihosseini, M. K., Drouin, J., Kaartinen, V., and Bellusci, S. (2008) *PLoS ONE* **3,** e1516
42. Mailleux, A. A., Kelly, R., Veltmaat, J. M., De Langhe, S. P., Zaffran, S., Thiery, J. P., and Bellusci, S. (2005) *Development* **132,** 2157–2166
43. Beer, H. D., Florence, C., Dammeier, J., McGuire, L., Werner, S., and Duan, D. R. (1997) *Oncogene* **15,** 2211–2218
44. Tomlinson, D. C., Grindley, J. C., and Thomson, A. A. (2004) *Endocrinology* **145,** 1988–1995
45. Yoo, Y. A., Kang, M. H., Kim, J. S., and Oh, S. C. (2008) *Carcinogenesis* **29,** 480–490
46. Dennler, S., Andre, J., Alexaki, I., Li, A., Magnaldo, T., ten Dijke, P., Wang, X. J., Verrecchia, F., and Mauviel, A. (2007) *Cancer Res.* **67,** 6981–6986